RSC Advances

PAPER

View Article Online
View Journal | View Issue

Cite this: *RSC Adv.*, 2026, **16**, 14216

Chitosan-based hydrogels: bentonite supported architectures explored for removal of cadmium(II) from aqueous solution

Zain Ul Abdeen Chaudhry, Nasima Arshad * and Muhammad Anees Ur Rehman Qureshi

To maintain ecosystem integrity, the use of hydrogels as adsorbents is a straightforward and cost-effective approach towards heavy metal removal from drinking water and wastewater. Heavy metal ions have lethal effects on all life forms by entering the food chain through the waste disposal in water channels. Among various metal ions, cadmium ion Cd(II) is at the top of the toxicity list. Herin, we report the synthesis and Cd(II) removal efficiency of chitosan-based hybrid hydrogel CPAB {chitosan (C)/poly(vinyl alcohol) (P)/3-aminopropyltriethoxysilane (A)/bentonite (B)}. Bentonite clay was used as a filler in four different amounts in CPAB-15, CPAB-30, CPAB-45, and CPAB-60 compositions. FTIR, SEM and XRD, and TGA characterization indicated structural, surface, and morphological modifications and significant enhancement in the thermal stability. Swelling analysis revealed that, in water, CPAB swells rapidly in the presence of bentonite. A gradual increase was observed as a function of bentonite concentration. In addition, these hydrogels showed better swelling in acidic pH. The prepared hydrogels were subjected to batch tests and experimental evidence revealed that CPAB-15 is the best composition for Cd(II) removal from water. The maximum percentage removal and equilibrium adsorption efficiency (q_e) results obtained from batch experiments are in-agreement and assured that 90 mg adsorbent dose adsorbed 25 mg of Cd(II) in 120 min at pH 6. Theoretical modelling indicated that the experimental data for Cd(II) removal was well fitted to Langmuir isotherm and pseudo-second order kinetic models. The adsorption kinetics revealed chemisorption to be the most probable adsorption process, while the equilibrium adsorption capacity (q_{max}) of 354.61 mg g^{-1} evaluated from the Langmuir model was found to be much greater than most of the reported chitosan-based hydrogels and endorsed the appropriateness of the CPAB-15 hydrogel to be used as an efficient adsorbent system for Cd(II) removal from water.

Received 20th January 2026
Accepted 9th March 2026

DOI: 10.1039/d6ra00503a

rsc.li/rsc-advances

1. Introduction

Heavy metal contamination in water presents serious environmental and health concerns, with Cd(II) ions being especially toxic and persistent. Conventional methods for water purification using various techniques such as membrane filtration, ion exchange, reverse osmosis, electrodialysis, *etc.* are encumbered with disadvantages involving high costs, inadequate efficiency, and environmental hazards; however, adsorption has been considered comparatively more advantageous than other used water purification techniques.[1–4] The adsorbents used by this technique have been reported not only for their cost effective and environmentally friendly attributes but also for effective and efficient removal of metal ions and other contaminants from wastewater.[5] A variety of adsorbent materials have been investigated in this scenario. Among them, hydrogels are considered the most versatile due to their excellent adsorption capability associated with their large surface area, high porosity, and the presence of functional groups which enhance their adsorption capacity.[6] Hydrogels effectively adsorb both inorganic and organic pollutants from water onto their surface through physical and chemical interactions.[7] In addition to adsorption, hydrogels can perform ion exchange with surrounding solutions, capturing heavy metals and other ionic pollutants through electrostatic interactions.[6,7] This mechanism is particularly significant for treating industrial wastewater, where ionic contaminants are prevalent. Ion exchange can enhance the selectivity of hydrogels for specific ions, optimizing their effectiveness in various applications.[8]

Hydrogels are three-dimensional polymer networks capable of holding large amounts of water, making them a promising technology in water treatment applications due to their high absorbency, adaptability, and the presence of hydrophilic sites like –COOH, –OH, $–NH_2$, $–CONH_2$.[9–13] Hydrogels are synthesized from hydrophilic polymers, which imbibe significant amount of water while maintaining their structural integrity.[14] This property renders hydrogels particularly effective in absorbing and

Department of Chemistry Allama Iqbal Open University, Islamabad, Pakistan. E-mail: nasimaa2006@yahoo.com; nasima.arshad@aiou.edu.pk

removing various contaminants from water like heavy metals, dyes and organic pollutants that could bind with hydrogels due to the availability of targeted hydrophilic sites.[15–17]

Based on their origin and composition, hydrogels are majorly categorized as natural, synthetic, and hybrid.[13] Natural hydrogels derived from biopolymers are mainly polysaccharides and include, but are not limited to, cellulose, chitosan, alginate, starch, hyaluronic acid, pectin, dextran, xanthan gum, agar *etc.* These hydrogels are environmentally friendly and biodegradable, making them an attractive option for sustainable water treatment solutions.[7,18,19] Synthetic hydrogels, made from synthetic polymers like polyacrylamide, poly(vinyl alcohol), and polyethylene glycol, offer tunable properties, high mechanical strength, and stability under various environmental conditions.[13,20] These characteristics allow for targeted applications where specific pollutant removal is required.[19] Hybrid hydrogels combine both natural and synthetic polymers to harness the advantages of both types and have been investigated frequently for various applications.[21–23] By integrating the biodegradability of natural polymers with the customizable properties of synthetic ones, hybrid hydrogels provide enhanced performance in pollutant removal and improved mechanical stability.[24]

Chitosan is derived from the exoskeletons of crustaceans such as pawn, crab, shrimp, green algae, and fungi.[25] Chitin serves as the parent polymer from which it is de-acetylated to yield chitosan.[26] This is justified because chitosan contains two –OH and one $–NH_2$ groups, which are responsible for its swelling, hydration, biodegradation, and gelation.[27] For this reason, it has been immensely used in the preparation of hydrogels, cryogels, and aerogels.[28,29] Chitosan-based hydrogels are particularly effective in adsorbing heavy metals due to the presence of amino and hydroxyl groups, which can chelate metal ions.[30] Synthetic polymers are preferred in hydrogel systems because they are more easily processed, degradable, modifiable, and have higher mechanical resilience. Hence, structural alteration of biopolymers is performed by crosslinking them with synthetic polymers to gain collective advantages and improved physicochemical properties.[31] Among various synthetic polymers, poly(vinyl alcohol), due to non-carcinogenicity and desirable swelling properties in water, has great importance in hydrogel synthesis.[32] Furthermore, it has excellent film-forming, adhesive, and emulsifying capabilities.[33]

The synthesis and performance of chitosan/poly(vinyl alcohol) hydrogels are greatly influenced by crosslinking agents. Glutaraldehyde and epichlorohydrin are widely used crosslinkers in wastewater. Regardless of excellent metal ion removal capabilities of hydrogels having these crosslinkers is still a question mark because of their toxic nature and could not be ignored while using them in water and living systems.[34] On the other hand, 3-aminopropyltriethoxysilane is a powerful silane coupling agent. It introduces amine groups that promote network stability and covalent bonding between polymeric matrices that enhance the structural and mechanical properties of hydrogels to be used in various applications.[20,35]

Despite the natural-synthetic polymer blending, hydrogels are mechanically weaker and have limited in uptake of metallic ions.[36] However, the addition of a filler, like natural clay, nanofiber, cellulose, graphene oxide, and metal oxide, increases the overall surface of hydrogels and promotes their interaction with metal ions.[37,38] For instance, incorporation of bentonite into hydrogel not only increases swelling capacity but also enhances the sorption capability to remove contaminants from wastewater and drinking water.[39]

Keeping in view the Cd(II) toxicity, an attempt is made in current work to synthesize new chitosan/polyvinyl crosslinked hydrogels by using varying amounts of bentonite clay as filler. Subsequently, these hydrogels were characterized and further investigated for Cd(II) adsorption.

2. Materials & methods

2.1. Chemicals

Following chemicals and reagents were used in current study. Chitosan (CAS No. 9012-76-4; MW: 190 000–310,000 g mol^{-1}, ≥75% deacetylation, bulk density 0.15–0.30 g cm^{-3} and viscosity > 200 centipoises), poly(vinyl alcohol) (CAS No.9002-89-5; MW: 30 000–70,000), 3-aminopropyltriethoxysilane crosslinker (CAS No. 919-30-2, 99%), and bentonite clay (CAS No. 1302-78-9) from Sigma-Aldrich, H_2SO_4 (CAS No.7664-93-9, M.W 98.08 g mol^{-1}), CH_3COOH (CAS No 64-19-7, M.W 60.05 g mol^{-1}), and NaOH (CAS 1310-73-2, M.W 40 g mol^{-1} from Merck, standard solution of cadmium (CAS No 7440-43-9, M.W 112.41 g mol^{-1}) from Scharlau, CH_3OH (CAS No 67-56-1, M.W 32.04 g mol^{-1}) from BDH, and Whatman Filter Paper (CAT No. 1442) from Schleicher and Schuell were purchased and used as received.

2.2. Synthesis of CPAB hydrogels

60 mL of 2% CH_3COOH was used to dissolve 1 g of chitosan. In another breaker,1 g of poly(vinyl alcohol) was dissolved in 40 mL of distilled water. Both solutions were then mixed and heated at 70 °C for 2 hours with continuous stirring. In the subsequent step, 0, 15, 30, 45, and 60 mg of bentonite was dissolved separately, in 5 mL of distilled water, sonicated for 1 hour, rested for one more hour, then added dropwise into the polymeric mixture. Subsequently, mixture was blended for 2 hours at 70 °C. 60 μL of crosslinker (3-aminopropyltriethoxysilane) was added in 10 mL of methanol and continuous stirring of this solution was done for 30 minutes. This solution was added into the blending mixture and stirred for another hour. The final mixture was poured in a Petri dish and left to dry at room temperature. The dried cast hydrogels were labeled with CPAB-0 (that lacks bentonite), CPAB-15, CPAB-30, CPAB-45, and CPAB-60. The synthesis steps and prepared hydrogels are provided in Fig. 1.

2.3. Characterizations – structure, morphology, and thermal stability

FTIR, XRD, SEM, and TGA were the characterization techniques used in this study. For structural analysis of synthesized hydrogels, FTIR spectrometer (Thermo Fisher Scientific's Nicolet iS10, Brookhaven, USA) was used. Initially, each sample was vacuum-dried, and its spectrum was obtained at the resolution of 2 cm^{-1} in the range of 4000–400 cm^{-1}. The surface

Fig. 1 Scheme for hydrogel synthesis and pictures of prepared CPAB hydrogels.

morphology was assessed using XRD (Xpert pro diffractometer, PANalytical Almelo, Netherlands) and SEM (MIRA3 TESCAN, Brno, Czech Republic). The Cu Kα radiations (λ: 1.544 Å), size of scanning step size (0.025°), and working range (2θ; 5°–80°) were used in XRD analysis. For SEM analysis, each hydrogel specimen was coated with tungsten at 0.8 nm s^{-1} for 92 second using a sputter coater (Safematic CCU-010), then connected to the carbon conductive tap, and examined at different magnifications. Thermal stability of each sample was checked by TGA instrument (Newcastle, USA, model Q50). 5 mg of the sample was placed in a Pt-pan and heated at 10 °C min^{-1} up to 700 °C. Nitrogen purging was done continuously at 40 mL min^{-1} to create an inert atmosphere.

2.4. Swelling analysis

To confirm the synthesized hydrogels' ability to swell, the swelling analysis was done in distilled water. Swelling behavior was observed, in triplicates, at room temperature. Initially, the weight of 10 mg of each dried hydrogel sample was measured, then added into the distilled water, the weight of each swollen hydrogel was recorded at predetermined time intervals. Prior to weighing, excess solvent was cleaned with the help of tissue paper. The swelling capacity of each hydrogel formulation was calculated using the following eqn (1).

$$\text{Swelling } (\%) = \frac{W_s - W_d}{W_d} \times 100 \quad (1)$$

where W_d represents the weight of the hydrogel represent in its dry state and W_s represents the weight of the hydrogels in swollen state. Following the same procedure, the hydrogel's swelling capabilities were further checked at the different pH solutions (pH 2–12) and their swelling % were calculated by using the same equation.

2.5. Adsorption studies

2.5.1. Preparation of stock solution. Adsorption studies were carried out to investigate the adsorption capacity of synthesized hydrogels for cadmium. The stock solution was

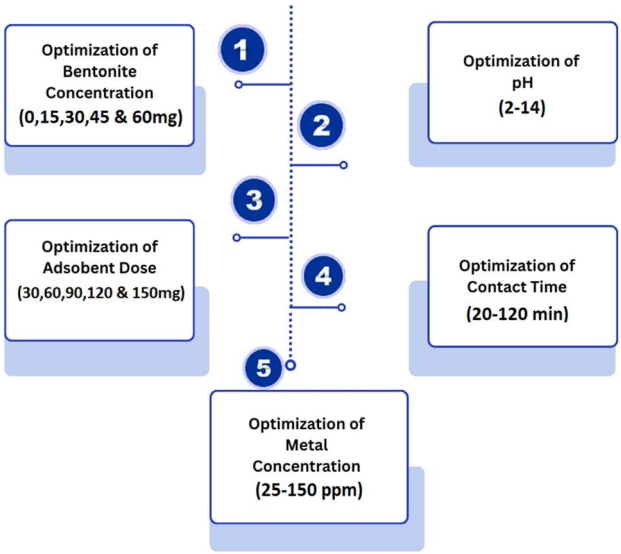

Fig. 2 Optimization steps in batch adsorption experiment.

prepared from the cadmium-certified reference material (CRM) of 1000 ppm; further dilution was made to prepare 100 ppm, 80 ppm, 60 ppm and 10 ppm solutions in 2% HNO_3 solution.

2.5.2. Batch experiments. The batch adsorption experiments were performed at different pH, contact times, and adsorbent doses. For the optimization of all parameters, the study was conducted in a stepwise manner and shown in Fig. 2. For bentonite concentration and pH optimization, 2 × 2 cm size piece of each prepared hydrogel sample with a weight of approximately 60 mg was placed in a 100 ppm cadmium standard solution for 20 min at pH 7 and at different pH (2–14), respectively. For optimizing contact time (20–120 min), hydrogel of optimum pH, absorbent dose, and bentonite concentration are placed at different time intervals and then, to find the most favorable metal concentration ion, place the hydrogels at different concentrations (25 ppm to 150 ppm) using a stock solution of cadmium. The equilibrium concentration of cadmium was found by atomic absorption spectrometer AAS (PerkinElmer Analyst 600) and the data was used in different adsorption isotherms and kinetic models. The determination of equilibrium adsorption capacity (q_e) and percentage removal (%) for all optimization parameters were calculated by using eqn (2) and (3), where C_i and C_f are the initial and final concentration of cadmium, W is the weight of hydrogel and V is volume of the metal ion concentration.

$$q_e = \left(\frac{C_f - C_i}{V}\right)W \quad (2)$$

$$\text{Percentage removal } (\%) = \left(\frac{C_f - C_i}{C_f}\right) \times 100 \quad (3)$$

2.5.3. Adsorption isotherms and adsorption kinetics. The two-adsorption isotherms models, Langmuir and Freundlich, were studied for the cadmium metal ions concentration ranging from 25–150 mg L^{-1} using the adsorbent dose of 90 mg/20 mL. Mathematical forms of Langmuir (eqn (4) and 5) and Freundlich (eqn (6)) adsorption isothermal models are provided below.

$$\frac{C_e}{q_e} = \frac{1}{q_{max}b} + \frac{C_e}{q_{max}} \quad (4)$$

$$R_L = \frac{1}{1 + bC_m} \quad (5)$$

$$\log\ q_e = \log\ K_f + \frac{1}{n}\log\ C_e \quad (6)$$

In Langmuir isotherm model equation, q_e is the equilibrium adsorption uptake of heavy metal ions, q_{max} is the maximum adsorption capacity corresponding to the full monolayer coverage, b is Langmuir constant and related to the adsorption energy, C_m is maximum starting concentration of heavy metal ions, and R_L is a dimensionless constant separation factor and its value *i.e.*, $R_L = 0$, >1, +1, and <1 represents that adsorption is irreversible, adverse, linear, and favorable, respectively. In Freundlich isotherm model equation, K_f and n are the two constants that are related to adsorption capacity of adsorbate and adsorption intensity, respectively.

The pseudo-first order and pseudo-second order models were employed to describe the adsorption kinetics, and their mathematical expressions are provided as eqn (7) and (8), respectively.

$$\log\ (\ q_e - q_t\ ) = \log\ q_e - \frac{k_1}{2,303}t \quad (7)$$

$$\frac{t}{qt} = \frac{1}{k_2 q_e} + \frac{t}{q_e} \quad (8)$$

where, q_e is equilibrium adsorption capacity (mg g^{-1}) at time t, k_1 and k_2 are pseudo-first order (min^{-1}) and is pseudo-second order (g mg^{-1} min^{-1}) rate constants, respectively.

3. Results and discussion

3.1. Synthesis

Five hydrogels, CPAB-0, CPAB-15, CPAB-30, CPAB-45, and CPAB-60, were prepared according to the scheme mentioned in Fig. 1 and the possible interactional mechanism is presented in Fig. 3. 3-Aminopropyltriethoxysilane was added at its optimal concentration of 60 μL in 10 mL CH_3OH to cross link the hydrogel components. This concentration of crosslinker was found to be best, while brittle hydrogels were obtained at other tried concentrations of 20–40 μL/10 mL CH_3OH. Only the variation in the filler (bentonite) was made in the hydrogels' formulation. The components and their exact amounts used in current hydrogels formulation are summarized in Table 1. Chitosan, a polysaccharide of glucosamine and *N*-acetyl glucosamine units, has hydroxyl (–OH) and amino groups (–NH_2) that establish intense hydrogen bonding with the hydroxyl groups of poly(vinyl alcohol) to give a compatible and tough polymer network.[40] Bentonite, as negatively charged layered silicate sheets, electrostatically interacts with protonated amino groups of chitosan to enhance network stability and adsorption properties.[41] Likewise, 3-aminopropyltriethoxysilane, with both

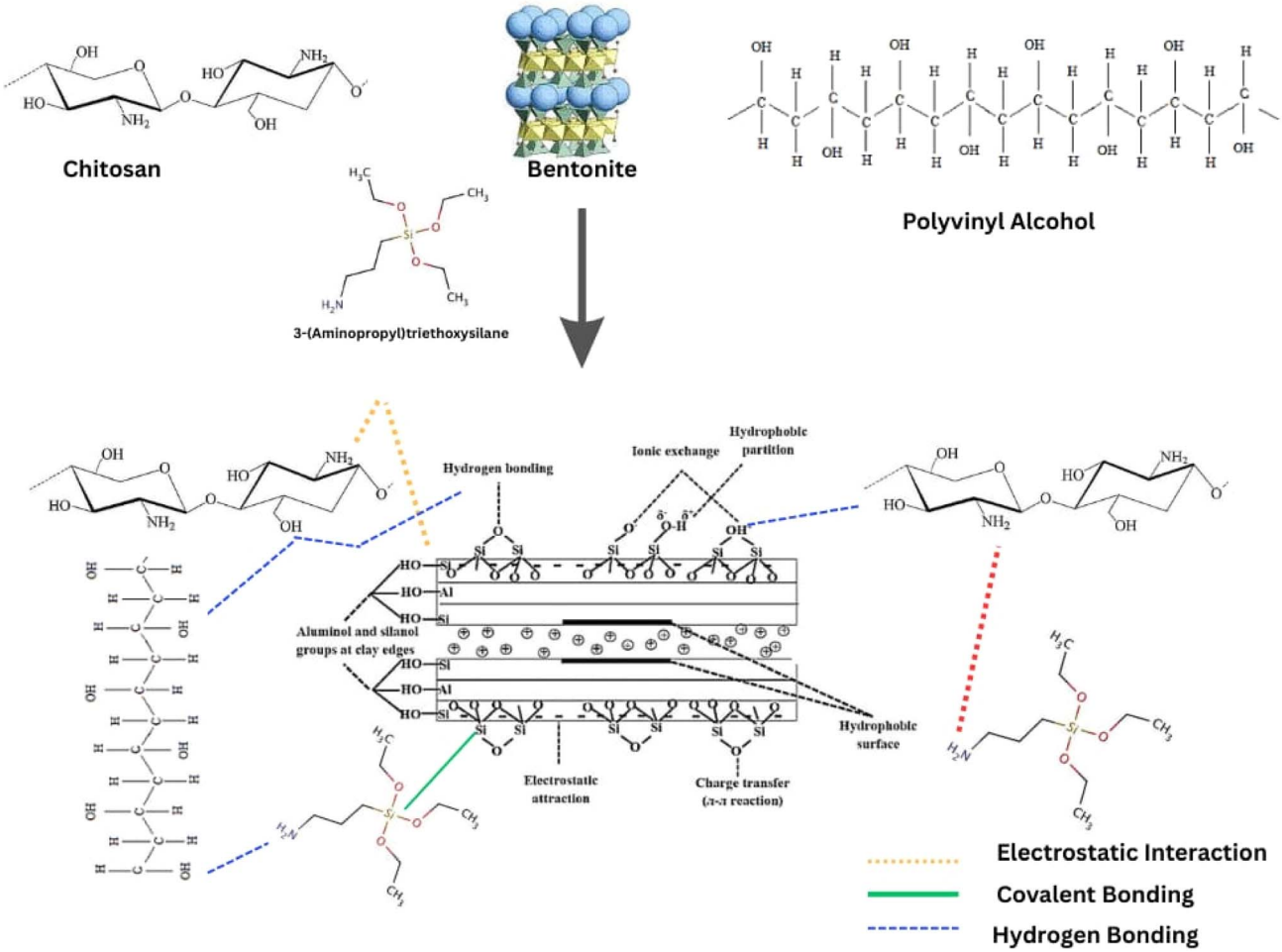

Fig. 3 A plausible interactional mechanism for the prepared hydrogels.

Table 1 CPAB hydrogels' compositions

	Composition			
Hydrogels	Chitosan (g)	Poly(vinyl alcohol) (g)	3-Aminopropyltriethoxysilane (μL)	Bentonite (mg)
CPAB-0	1.0	1.0	60	0.0
CPAB-15	1.0	1.0	60	15
CPAB-30	1.0	1.0	60	30
CPAB-45	1.0	1.0	60	45
CPAB-60	1.0	1.0	60	60

silane and amino groups, establishes covalent linkages with bentonite through its silane units and interacts with chitosan/poly(vinyl alcohol) through its amino group to additionally crosslink the matrix.[42] Hydrogels of higher mechanical strength, barrier property, and adsorption capability are obtained through hydrogen bonding, covalent, and electrostatic interactions to impart suitability for uptake of heavy metal.

3.2. Physical characterization

3.2.1. FTIR. The overlay of FTIR spectrum of formulated hydrogels (CPAB-0, −15, −30, −45, −60) and a comparative FTIR overlay of metal adsorbed hydrogel (MCPAB) are provided in Fig. 4(a and b). The FTIR region at 3265–3305 cm^{-1} indicated the presence of hydroxyl and amine groups this range and correlates to O–H and N–H stretching vibrations within chitosan, bentonite and poly(vinyl alcohol). Potential hydrogen bonding interactions inside the hydrogel are suggested by these functional groups.[43] The region around 2919–2973 cm^{-1} is attributed to C–H stretching vibrations, which correspond to aliphatic C–H bonds. Chitosan and poly(vinyl alcohol) have been reported to contain methylene and methyl groups, which contribute to the overall hydrophobic character of the

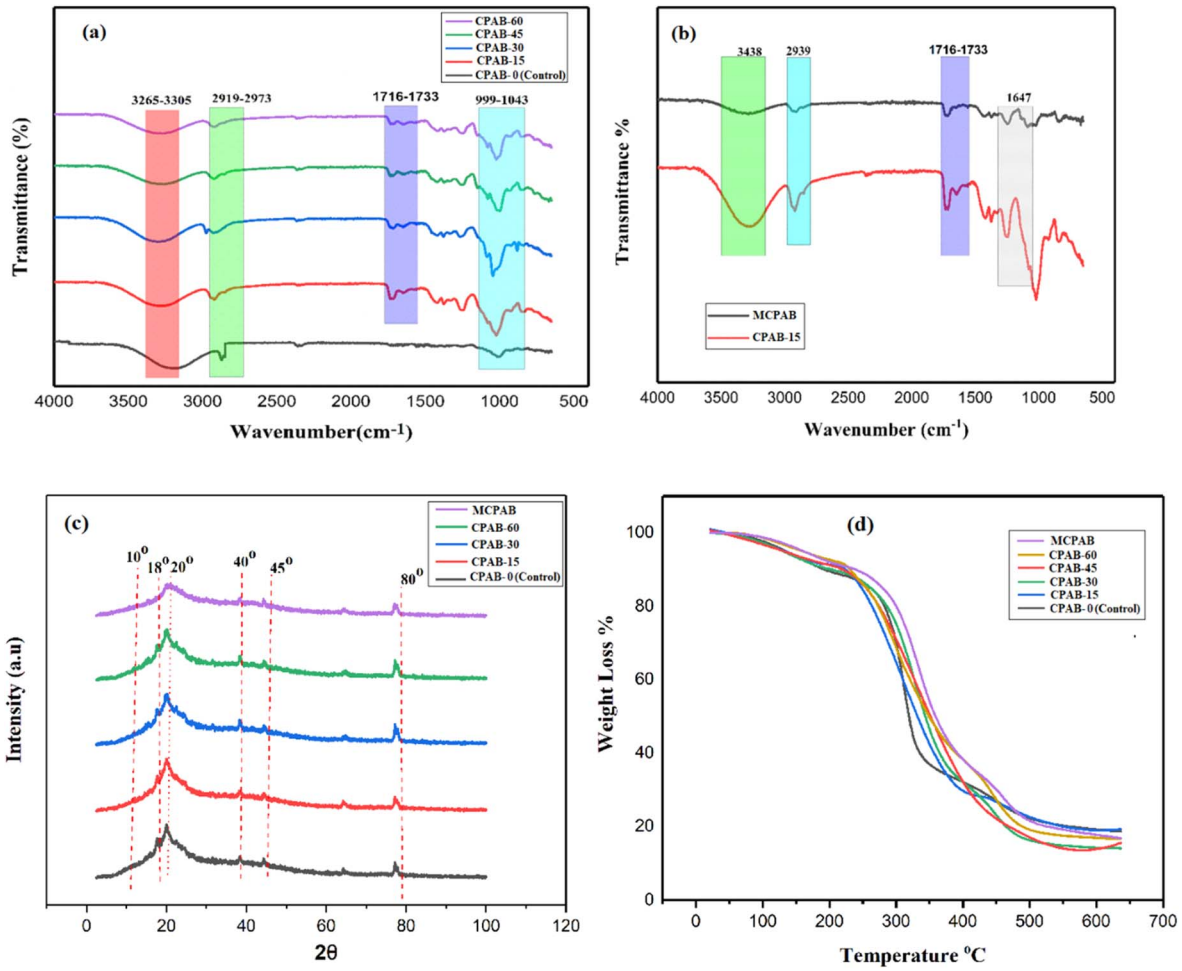

Fig. 4 (a and b) FTIR overlay spectrum, (c) XRD patterns, and (d) TGA thermograms of prepared hydrogels before and after Cd(II) adsorption.

hydrogel.[44] Carbonyl groups responsible for the C=O stretching is observed within 1716–1733 cm^{-1} range which are most likely from poly(vinyl alcohol) or acetylated chitosan.[45] This identifies possible sites for cross-linking in the hydrogel network. C–O and C–N stretching vibrations in the range of 1043 cm^{-1} to 999 cm^{-1} are indicative of ether/alcohol (C–O) and amine (C–N) groups.[46] The presence of carbonyl groups interacting with cadmium ions may be indicated by the peak at 1645 cm^{-1} (C=O stretching), which could indicate complexation or coordination between the metal ion and the carbonyl oxygen. The very common aliphatic C–H stretching in most organic compounds appears as the peak positioned at 2923 cm^{-1}. Its presence demonstrates that, under conditions of adsorption, the components of organic hydrogels may bind with cadmium ions. The O–H stretching peak at 3438 cm^{-1} is indicative of free hydroxyl groups which can interact with cadmium ions during adsorption *via* ionic or hydrogen bonding interactions.[47,48]

3.2.2. XRD. XRD could help in assessing the structural characterization of hydrogel-based adsorbents for the removal of heavy metals from aqueous solutions. The XRD patterns are provided in Fig. 4c and demonstrated the major phases associated with bentonite, poly(vinyl alcohol), and chitosan. The characteristic peaks of chitosan appeared at approximately $2\theta = 10°$ and 20°, while poly(vinyl alcohol) exhibited peaks at about $2\theta = 18°$ and 22°.[49] The incorporation of bentonite into the hydrogel matrix was evidenced by the presence of well-defined peaks at around $2\theta = 7.1°$ and 20°. The diffraction peak at $2\theta = 7.1°$ is indicative of interaction of hydrogel's constituents with bentonite *via* intercalation into the layered structure of bentonite,[50] while the peak at diffraction angle of $2\theta = 20°$ represents a characteristic peak of bentonite which corresponds to the plane (110).[51] The presence of discreet peaks within 2θ range of 40–45° and 60–80° in the XRD patterns further indicated crystallinity in the prepared hydrogels' structure.[52] Such structural integrity is essential for the mechanical properties of the hydrogels to be used in adsorption applications.[53] Interactions of chitosan and poly(vinyl alcohol) reduce the overall crystallinity by enhancing amorphous content through broadening and decreasing of the intensity of its peaks, whereas addition of bentonite increased the crystallinity and interlayer spacing in a composite, resulting in enhanced peak intensity and emergence of supplementary peaks in XRD pattern.[54,55] This enhancement may translate to improved heat stability and mechanical properties.[56] Adsorption of heavy metals hardly

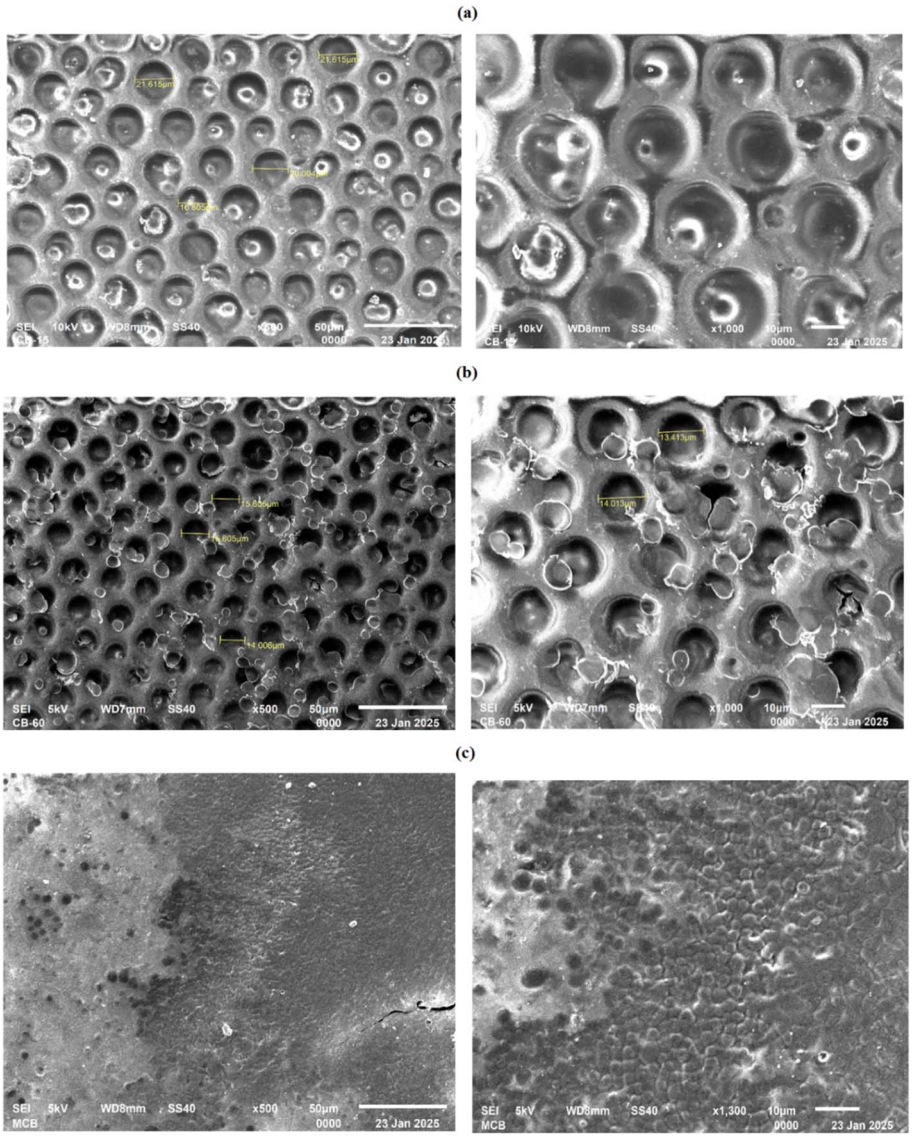

Fig. 5 SEM images of (a) CPAB-15, (b) CPAB-60, and (c) MCPAB at different magnifications.

affects the composite's crystallinity because the XRD patterns indicate limited change after adsorption.[57] It also suggests that functional groups within the hydrogel matrix interacted with cadmium ions. To enhance the binding capacity for cadmium ions, this interaction may involve coordination or complexation with hydroxyl or amino groups present in chitosan and crosslinker.[58]

3.2.3. TGA. Thermal stability of hydrogel-based adsorbents, for metal/other contaminants removal from wastewater, is also an important factor and directly influences its structural integrity and adsorption capability.[59] Thermograms of all prepared hydrogels are provided in Fig. 4d. Thermogravimetric analysis (TGA) showed almost 100% mass retention up to around 100 °C, indicating low moisture content and good thermal stability at lower temperatures. The control hydrogel (CPA) started degrading at around 221.38 °C, thus providing a baseline to compare the modified hydrogels (CPAB-15, CPAB-30, CPAB-45, and CPAB-60). Hydrogels containing different amounts of bentonite displayed enhanced thermal resistance, with the start of mass loss shifted to somewhat higher temperatures with increased bentonite content. It may thus be inferred that bentonite increases the thermal stability of the hydrogel matrix. All (CPAB) samples showed a final mass residue of about 16% at temperatures around 600 °C, suggesting that after the thermal degradation process, a large part of the material was retained. TGA indicated the degradation of polymer chains and functional groups in chitosan and poly(-vinyl alcohol) that occurred between 200 and 300 °C in CPAB-0 hydrogel (control). The loss of such important functional groups during the degradation process would obviously affect the adsorption ability.[60] However, the presence of bentonite in modified hydrogels (CPAB-15 to 60) seems to counteract this effect due to its structural durability, which may lead to an improved adsorption capacity.[61] The elevated breakdown

temperature and mass retention confirmed that structural changes, due to bentonite, enhanced the thermal stability of CPAB hydrogels.[62] The observed weight loss in CPAB hydrogels at high temperature may be due to some breakdown in alkyl chains in hydrogel's moieties that are covalently bonded to the bentonite.[61] The metal-adsorbed hydrogel (MCPAB) was found to retain its mass constantly throughout the studied temperature range as compared to CPAB analogs. The elevated thermal stability and mass retention in the MCPAB could be attributed to metal ion interaction with the functional groups (*e.g.*, –OH, –COOH, $–NH_2$), hence coordinated metal further strengthens the hydrogel network.[63]

3.2.4. SEM. The SEM images at different magnification are presented in Fig. 5. SEM images indicated that the hydrogels exhibited uniform circular pores and channelized networks, which are critical for applications requiring high porosity for mass transfer adsorption processes. For the hydrogel sample with a bentonite concentration of 15 and 60 mg, the measured pore sizes were found to be approximately in the range of 16–21 and 14–15 μm, respectively, Fig. 5(a and b). This suggested a favorable porosity that can facilitate the adsorption of contaminants from wastewater.[64] The reduction in pore size with increased bentonite concentration may indicate a denser network formation that potentially enhanced the mechanical stability but can minimize the surface area. Small pore size may hinder the influx of larger molecules or ions to cause pore clogging; hence making it less efficient for adsorption of contaminants into the hydrogel linkages.[65] While, with comparatively large, even, and circular pore size, CPAB-15 sample showed a heterogeneous surface morphology and multidimensional structural spots which are indicative of expended surface area. This may channelize the network to allow for easier diffusion and capture of metal ions such as Cd(II). After cadmium metal loading, the hydrogel sample with 15 mg of bentonite showed a heterogeneous surface with tiny round holes and multidimensional structural spots. Because it expands the surface area accessible for contact with pollutants, this heterogeneous morphology is advantageous for adsorption applications. This accessibility to trap metal ions results in improving adsorption capacity diffusion rate of a hydrogel.[66]

3.3. Swelling analysis

Hydrogels' swelling is a time dependent absorption process. Swelling behavior relies on the ionic functional groups, cross-linkers, monomeric entities, and porous hydrophilic networks in hydrogels' structures. Hydrogels with such characteristics could be employed as excellent adsorbent for toxicant removal from wastewater.[67] Swelling of each prepared hydrogel was checked in distilled water and at different pH values. The evaluated percentage swelling of each hydrogel is graphically represented in Fig. 6(a and b). The increase in swelling was observed steeper during initial time intervals that gradually slowed down till an equilibrium was reached. This swelling behavior could be attributed to the porous and layered structure of hydrogels due to which the swelling ratio increases longitudinally and typically reaches a plateau as the network becomes saturated.[68]

The percentage of swelling in distilled water was noted at various time points, Fig. 6a, which demonstrate that swelling rises with time in all hydrogel formulations. A gradual increase in swelling, in almost all the hydrogel samples, was observed by 120 minutes. However, observing 30 more minutes, the swelling in CPAB-0, CPAB-15, CPAB-30, CPAB-45, and CPAB-60 was found to increase from 133% to 769%, 294 to 1215%, 479 to1726%, 641 to 2046%, and 839 to 2459%, respectively. Based on the results, the hydrogels with bentonite concentrations had greater, while hydrogel without bentonite (CPAB-0) had lowest swelling capacity at the end of the observation time. The huge surface area and water-holding capacity due to bentonite's layered structure are responsible for this improvement.[69] However, among all CPAB hydrogels, CPAB-60 exhibited highest swelling which indicated that swelling was strongly influenced by the bentonite content in the hydrogel matrix.

Swelling behavior of prepared hydrogels at different pH solutions are presented in Fig. 6b. For most of the hydrogels, especially those with a higher bentonite content, the percentage

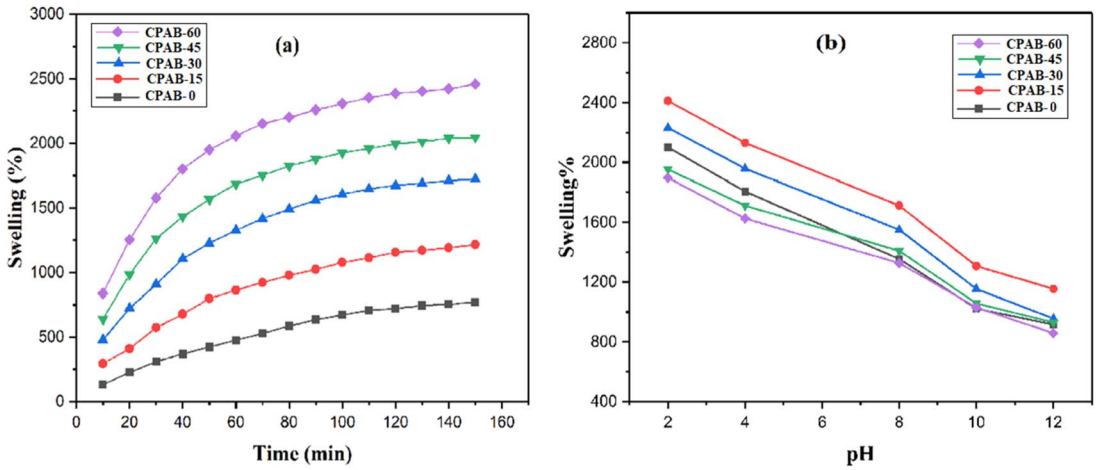

Fig. 6 Swelling percentage of each prepared hydrogel in (a) distilled water with respect to time, and (b) at various pH values.

swelling was observed to be comparatively higher at low pH values. The maximal swelling was estimated to be 1753%, 2474%, 2143%, 1844%, and 2384% for CPAB-0, CPAB-15, CPAB-30, CPAB-45, and CPAB-60, respectively, at pH 2. The swelling rise at low pH values for chitosan/poly(vinyl alcohol) hydrogels is largely a consequence of protonation of the amine groups ($-NH_2$) into ammonium groups ($-NH_3^+$) in acidic environment.[70–72] These positive charges, *via* distribution along polymeric backbone, opened-up its network and as a result hydrogels' hydrophilicity was boosted. Further, presence of ($-NH_3^+$) at low pH causes electrostatic repulsion and drop in the osmotic pressure which led to increased swelling.[70] On contrary, de-protonation of ($-NH_3^+$) at high pH values decreased the interactions within polymeric network and caused the polymer chain to contract. Hence a more compact polymer network restricted the chain mobility and water uptake and resulted in decreased swelling in neutral and basic pH.[70–72] The presence of bentonite's layered structure further helps to increase the ion exchange capacity and surface area, which would enhance the water absorption affinity.[67,73]

3.4. Adsorption studies for Cd(II) removal

The adsorption studies for Cd(II) removal from water were conducted *via* batch tests and effects of bentonite concentration, pH, adsorbent dose, contact time, and Cd(II) concentration were investigated. The effect of bentonite concentration on Cd(II) adsorption was observed by placing 60 mg piece of each hydrogel (CPAB-0, −15, −30, −45, and −60) in cadmium standard 100 ppm solution, while keeping all other parameters constant (*i.e.*, pH 7; time 20 minutes). All bentonite-containing hydrogels performed better than the bentonite-free CPAB-0 hydrogel. Spectroscopic analysis revealed comparatively better adsorption of Cd(II) on CPAB-15 hydrogel sample, while further increases in bentonite (CPAB-30–CPAB-60) gradually decreased both Cd(II) removal percentage (% adsorption) and equilibrium adsorption capacity (q_e). The reason being the more porous structure of hydrogel matrix if bentonite concentration is lower that may have provided better access to adsorption sites and develop strong affinities for metal ions *via* amino and hydroxyl groups.[74,75] These functional groups present in the hydrogel composite are envisaged to contribute remarkably to metal adsorption.[76] While excessive bentonite may result in aggregation or diffusion limitations.

The effect of bentonite concentration on Cd(II) adsorption can be explained with the support of SEM, XRD, and TGA results. SEM studies (Fig. 5), showed that CPAB-15 has large, evenly distributed circular pores (16–21 μm) with heterogeneous surface topography. In contrast, CPAB-60 had much smaller pores (14–15 μm) and a more compact structure. This morphological change has a direct effect on adsorption capacity. Excess bentonite particles clog the interstitial spaces of the polymer matrix, causing physical pore channel blocking and thus decrease in accessibility of the cadmium ions. Literature also supported such findings where high clay content causes particle aggregation and pore blocking and thereby restricting diffusion channels for metal ions.[73,74,77] Hence decreasing the effective surface area and low to moderate bentonite loading may have maximized the availability of active adsorption sites.[62,73,74] At higher concentrations, bentonite particles are prone to aggregation in the chitosan-based matrix as obvious from XRD analysis. This affects the overall dispersion of clay platelets, resulting in a lower number of accessible active sites and causes self-aggregation, which decreases the interlayer distance for metal ion intercalation. The bentonite peak at $2\theta = 7.1°$ indicates intercalation, but peak broadening and changes in intensity at higher concentrations of bentonite indicate possible stacking disorder and agglomeration. TGA analysis (Fig. 4d), further revealed that higher concentrations of bentonite improve thermal stability, indicating a more compact, tightly cross-linked network. Although this is desirable for mechanical properties but makes it difficult for Cd(II) ions to diffuse into the binding sites. Adsorption is then mostly limited to the surface of the hydrogel, reducing overall equilibrium capacity (q_e).

The pH effect was monitored by using a pH range of 2–14. CPAB-15 hydrogel was placed, separately, in different pH solutions for 30 minutes and Cd(II) concentration was measured. Comparatively greater adsorption was measured in acidic environment. It could be attributed to protonation of amino ($-NH_2$) groups on chitosan into $-(NH_3^+)$ and increased porosity, surface area, and active adsorption sites of bentonite that may have promoted the Cd(II) complexation with hydrogel's network.[78,79] From swelling study (Fig. 6b), it is clear that the CPAB hydrogels have a maximum swelling capacity at acidic pH (up to 2474% for CPAB-15 at pH 2), which gradually decreases with increasing pH values towards neutral and basic regions. Simultaneously, from our batch adsorption studies (Fig. 7b and Table 2), the maximum Cd(II) removal was observed at pH 6. At low acidic pH values (pH 2–4), high degree of electrostatic repulsion between the polymer chains results in a swollen network structure because the H_3O^+ ions are abundant and very aggressively compete with Cd(II) ions for the available binding sites on the negatively charged bentonite surfaces. As a result, although the hydrogel is highly swollen, the adsorption capacity is low due to the occupation of binding sites by H_3O^+ ions. A favorable equilibrium is achieved at pH 6 because the amine groups are partially deprotonated, reducing electrostatic repulsion and hence the degree of swelling, which is lower than that at pH 2. However, this pH is below the pK_a value of chitosan (~6.5), which means there is a sufficient concentration of $-NH_3^+$ groups to ensure network hydrophobicity and swelling, although H_3O^+ competition is reduced. This allows Cd(II) ions to interact with both the amine groups of chitosan and the interlayer sites of bentonite.[80] This is supported by our experimental results, which show that CPAB-15 at pH 6 has high swelling (>1500%) and maximum q_e (98.89 mg g^{-1}). Conversely, at higher pH values, the $-NH_3^+$ groups are deprotonated to $-NH_2$, which causes network contraction and a consequent reduction in swelling, Fig. 6b. Additionally, low adsorption of Cd(II) ions at high pH levels could be associated with its precipitation and formation of cadmium hydroxide where hydroxide ions compete with the free Cd(II) ions for adsorption sites that decreases the removal

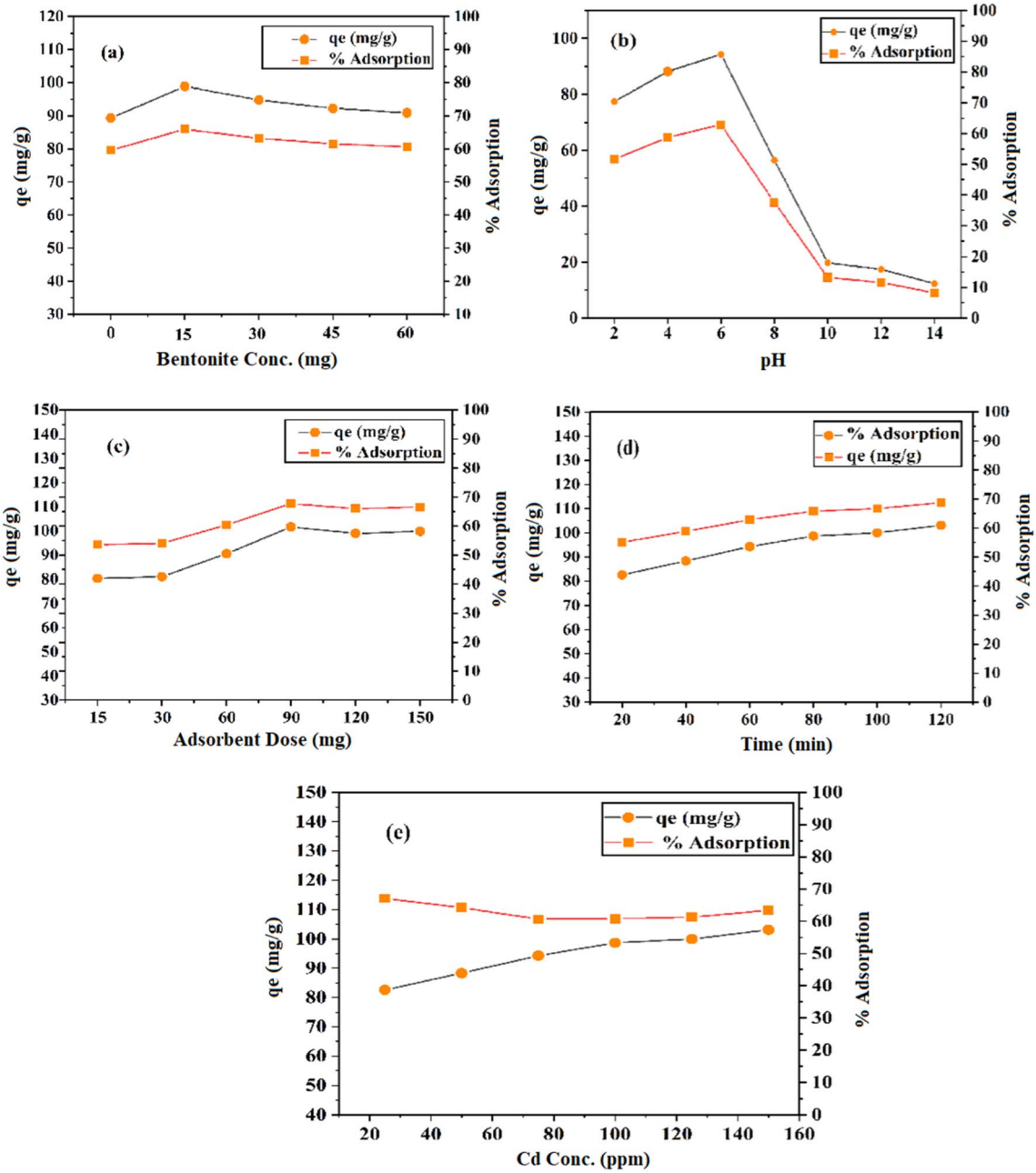

Fig. 7 Effect of (a) bentonite concentration, (b) pH, (c) adsorbent dose, (d) contact time, and (e) Cd(II) concentration and the evaluation of Cd(II) removal percentage and equilibrium adsorption capacity.

Table 2 Adsorption parameters elucidated from batch experiments

	Batch tests				
Adsorption parameters	Bentonite conc. (15 mg)	pH (6)	Adsorbent dose (90 mg)	Contact time (120 min)	Cd(II) conc.(25 mg)
% Adsorption	65	62.88	67.75	68.77	67.02
q_e (mg g^{-1})	98.89	98.89	101.62	103.15	103.14

percentage.[81] The two mechanisms, therefore, contributed to the sharp decrease in removal efficiency above pH 8. Industrial wastewater containing cadmium has a pH range of 5–8. Current results showed that CPAB-15 is specifically tailored for this purpose: it has sufficient pH-dependent swelling to ensure an accessible network.

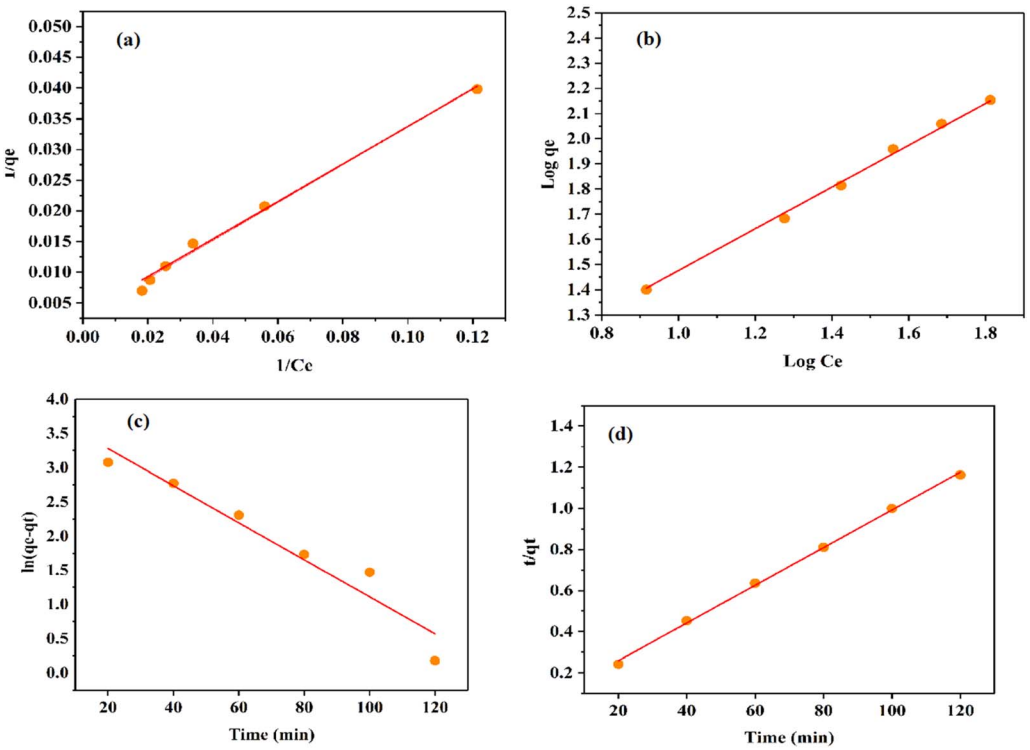

Fig. 8 Graphical representations of (a) Langmuir adsorption isotherm and (b) Freundlich adsorption isotherm, (c) pseudo-first order, and (d) pseudo-second order kinetic models.

15, 30, 60, 90, 120, and 150 mg pieces of CPAB-15 hydrogel were socked in 100 ppm cadmium standard solution for 30 minutes at pH 6 to check the effect of adsorbent dose on Cd(II) adsorption. The greater adsorption was observed above 60 mg adsorbent dose which indicated the availability of more active sites as adsorbent concentration goes higher. A slight decrease in the q_e values at higher doses (120, 150 mg) indicated that hydrogel reached its saturation point up to 90 mg and an equilibrium may be established between the adsorbent and free ions that may have limited the overall adsorption process.[82,83] This could further be attributed to the possibility of particles' agglomeration at increased doses, thereby reducing the surface area that is effectively available and leading to overlapping of adsorption sites, leaving them inaccessible.[84] Effect of Cd(II) concentration on removal efficiency and adsorption capacity indicated a rise in q_e but a slight drop in the removal efficiency as Cd(II) concentration increased. This could be attributed to the saturation of binding sites available on the surface of the hydrogel and cannot accommodate more Cd(II) ions hence reducing the percentage adsorption.[85]

The effect of bentonite concentration, pH, adsorbent dose, contact time, and Cd(II) removal concentration of all prepared hydrogels are shown in Fig. 7 (a–e), while maximum elucidated % adsorption and q_e values are provided in Table 2. Both adsorption parameters obtained from each batch experiment are almost unanimous and found to be in the ranges of 63–69% and 99–103 mg g^{-1}, respectively.

3.5. Isothermal and kinetic models' studies

The equilibrium data for Cd(II) removal from the CPAB-15 hydrogel were analyzed using Langmuir and Freundlich isotherm models, which give valuable information about the adsorption mechanism and capacity. The respective graphs and data are provided in Fig. 8(a, b) and Table 3. Both models were found to be well fitted with the data with comparatively more pronounced value of regression (R^2) obtained from Langmuir model. Although both models are excellent, the slight advantage of the Langmuir model, combined with physical validity, makes it the better model.

The Langmuir model considers monolayer adsorption on a surface with finite, equivalent, and evenly distributed binding sites. The CPAB-15 hydrogel provides a heterogeneous surface where Cd(II) ions selectively bind to carboxyl, hydroxyl, and amine functional groups, as well as negatively charged interlayer regions of the exfoliated bentonite.[86] The excellent Langmuir fit indicates a single-layer Cd(II) adsorption on these unique sites without any additional multilayer formation in our experimental setup. This is consistent with chemisorption (as indicated by pseudo-second-order kinetics), where strong site-specific interactions prevent additional layer formation due to limited binding sites. The maximum adsorption capacity (q_{max} = 354.61 mg g^{-1}) obtained from the Langmuir model represents a finite, saturable quantity—the total number of available binding sites in the hydrogel. This is a physical explanation. In contrast, the Freundlich constant (K_F) is empirical, and its units depend on the value of the exponent ($1/n$), making it more

Table 3 Adsorption isotherms and adsorption kinetics parameters for Cd(II) removal

Adsorption isotherms models						
	Langmuir			Freundlich		
Adsorbent CPAB-15	q_{max} (mg g^{-1})	K_L (L mg^{-1})/R_L	R^2	K_F (mg g^{-1}) (L mg^{-1})$^{1/n}$	n	R^2
	354.61	0.009/0.523	0.992	1.007	3.27	0.983
Adsorption kinetics models						
	Pseudo-first order			Pseudo-second order		
Adsorbent CPAB-15	q_{max} (mg g^{-1})	K_f (min^{-1})	R^2	q_{max} (mg g^{-1})	K_s (g mg^{-1}.min)	R^2
	45.73	0.027	0.937	109.00	0.001	0.988

difficult to assign a physical explanation. The Freundlich model describes surface heterogeneity with an exponential distribution of site energies, which is appropriate for natural sorbents but less consistent with the engineered, cross-linked hydrogel of CPAB-15. The favorability of adsorption is also confirmed by the dimensionless separation factor R_L from the Langmuir model. For CPAB-15, the R_L factor between 0 and 1 indicates a favorable adsorption process, providing additional thermodynamic support to the Langmuir model selection.

The theoretically evaluated value of maximum adsorption capacity (q_{max}) was found to be extremely high than that of several reported chitosan-based adsorbents, as an example, the q_{max} of modified chitosan-coated bentonite, bentonite with dispersed chitosan hydrogel, polyacrylic acid–chitosan hydrogel, surfactant–modified chitosan beads, graphene oxide–chitosan–poly(vinyl alcohol) hydrogel, chitosan–itaconic acid hydrogel, tripolyphosphate cross-linked chitosan, and natural hydroxyapatite/bentonite composite were reported to be 217.4, 168.70, 234.84, 125, 172.00, 285.70, 109.89, and 125.47 mg g^{-1}, respectively, which are 137.21, 185.91, 119.77, 229.61, 182.61, 68.91, 244.71, and 229.14 mg g^{-1} times lesser than that obtained for current hydrogel (CPAB-15).[75,78,79,85,87–90] This comparison underlines the suitability of CPAB-15 as an efficient adsorbent for cadmium removal from aqueous solution. The current findings suggest that the combination of poly(vinyl alcohol) with chitosan increases mechanical stability and introduces more hydroxyl groups, increasing active site density, while the layered structure and surface functionalities of bentonite within hydrogel network allow strong chemical interactions with Cd(II), *viz.* surface complexation and ion exchange through the –OH, –NH_2, and PO_4^{3-} groups.[91] Freundlich model parameter (n > 1) also suggested that adsorption is a very favorable process.

To investigate the rate and mechanism of Cd(II) adsorption onto the CPAB-15 hydrogel, experimental data was fitted into pseudo-first order and pseudo-second order kinetic models. The pseudo-first order kinetic theory assumes the adsorption process takes place by physisorption, and the rate is determined by the difference between the equilibrium and the current instant adsorption capacity. The pseudo-second-order model explains chemisorption comprising valence forces by electron sharing or electron transfer and the rate is directly proportional to the square of the difference from the equilibrium expression. The respective graphs and parameters are provided in Fig. 8(c, d) and Table 3. The regression (R^2) values obtained in both models are found to be > 0.90, but with comparatively high value for pseudo-second order, revealed it to be the best fitted model and assured that the rate-limiting step is probably chemisorption and involves valence forces through the sharing or exchange of electrons between Cd(II) ions and functional groups on the surface of the adsorbent.[91,92] The maximum adsorption capacity (q_{max}) evaluated by data fitting in pseudo-first order model was found to be quite less than that obtained from pseudo-second order model.

3.6. Selective sorption

Chitosan-based adsorbents have also shown remarkable selectivity for Cd(II) ions compared to other co-existing metal ions such as Pb(II), Ni(II), and others in complex aqueous environments due to their unique chelating properties. For example, chitosan-methacrylic acid (CS-MAA) nanoparticles have shown high selectivity for Cd(II), Pb(II), and Ni(II) ions in multi-ion aqueous environments due to their high coordination tendency.[93] Similarly, guanidine-modified poly(AMPSG/AAc/NVP/HEMA) hydrogels have also shown high selectivity for Cd(II) in the presence of Hg(II), Pb(II), Au(III), and others in aqueous environments, and their high capacity for efficient monolayer adsorption was explained using Langmuir isotherms, confirming the role of sulfonic and carboxylic groups in the selective adsorption of Cd(II).[94] Likewise, chitosan-Fe_3O_4-fish bone charcoal composites have selectively adsorbed Cd(II) ions from complex aqueous environments, and their adsorption capacity was found to be 64.31 mg g^{-1}, which is 1.7 times higher than biochar, and this high selectivity was due to their unique ion exchange, complexation, and electrostatic properties, even in the presence of co-existing metal ions.[95] Hence, based on reported literature, it could be inferred that the

modified chitosan-based hydrogel CPAB-15 in current studies have high selectivity for Cd(II).

4. Conclusions

CPAB-15, CPAB-30, CPAB-45, and CPAB-60 were prepared from pristine CPAB-0 hydrogel by varying bentonite concentration. Bentonite has not only improved the structural, morphological, and swelling properties of hydrogel but also extended its adsorption capacity for Cd(II) removal from aqueous solution. The structural integrity, surface morphology, crystallinity, and thermal stability was assured by FTIR, SEM and XRD, and TGA analysis and revealed appropriateness of current hydrogels to be used as adsorbent. With increased bentonite concentrations, the hydrogels showed remarkable swelling ratios of up to 2459%, demonstrating their ability to efficiently adsorb pollutants. Adsorption tests indicated that after one hour of contact time, hydrogels with lower bentonite concentrations (CPAB-15) exhibited 67% of Cd(II) removal at pH 6. The adsorption capacity (q_e) is main adsorption parameter that was evaluated both experimentally and by fitting the data in adsorption and kinetic models. The experimental results agreed indicating that at optimal conditions (15 mg bentonite, pH 6, 90 mg adsorbent dose, 120 minutes contact time, and 25 ppm Cd(II) concentration), CPAB-15 hydrogel favored Cd(II) adsorption. Maximum adsorption capacity (q_{max}) of 354.61 mg g^{-1} is achieved for CPAB-15 in current work *via* fitting the data in Langmuir isotherm adsorption model. The dominance of the Langmuir isotherm along with the pseudo-second order kinetic model specified chemisorption as the major mechanism of Cd(II) removal. The experimental and theoretical findings in terms of efficiency, kinetics, and adsorption mechanism highlight the effectiveness of current hydrogel system for Cd(II) adsorption. The hybrid approach in current work represents a breakthrough toward the development of cost-effective, environmentally friendly adsorbents and may seek attention especially where these materials are intended for practical use in water treatment. Further work on reusability may help to ensure the full characterization of explored hydrogel systems.

Author contributions

Zain Ul Abdeen Chaudhry: data curation, investigation, formal analysis, software, writing – original draft, writing – review & editing; Nasima Arshad: conceptualization, project administration, supervision, methodology, visualization, validation, resources, writing – original draft, writing – review & editing; Muhammad Anees Ur Rehman Qureshi: methodology, validation.

Conflicts of interest

There are no conflicts to declare.

Data availability

All required data supporting the findings are available in the manuscript. However, if any additional data is required, it will be made available on request.

Acknowledgements

Department of Chemistry, Allama Iqbal Open University, Islamabad Pakistan is highly acknowledged for all possible research facilities.

References

1 S. Satyam and S. Patra, Innovations and challenges in adsorption-based wastewater remediation: A comprehensive review, *Heliyon*, 2024, **10**(9), e29573, DOI: 10.1016/j.heliyon.2024.e29573.
2 H. Lu, D. Fu, X. Tai, Z. Sun and X. Wang, Metal–Organic Frameworks/Covalent–Organic Frameworks-Based Materials in Organic/inorganic Pollutant Elimination and CO2 Reduction Applications, *ChemNanoMat*, 2025, **11**(9), e202500244, DOI: 10.1002/cnma.202500244.
3 X. Pan, J. Ji, N. Zhang and M. Xing, Research progress of graphene-based nanomaterials for the environmental remediation, *Chin. Chem. Lett.*, 2020, **31**(6), 1462–1473, DOI: 10.1016/j.cclet.2019.10.002.
4 M. Xiao, X. Zhang, X. Liu, Z. Chen, X. Tai and X. Wang, Recent Progress in Covalent Organic Framework-Based Membranes: Design, Synthesis, and Applications in the Fields of Energy and the Environment, *ACS Macro Lett.*, 2025, **14**(8), 1201–1220, DOI: 10.1021/acsmacrolett.5c00403.
5 M. Akhtar, M. Sarfraz, M. Ahmad, N. Raza and L. Zhang, Use of low-cost adsorbent for wastewater treatment: Recent progress, new trend and future perspectives, *Desalin. Water Treat.*, 2025, **321**, 100914, DOI: 10.1016/j.dwt.2024.100914.
6 L. Alsaka, L. Alsaka, A. Altaee, S. J. Zaidi, J. Zhou and T. Kazwini, A review of hydrogel application in wastewater purification, *Separations*, 2025, **12**, 51, DOI: 10.3390/separations12020051.
7 A. Pattnaik, P. Ghosh and A. K. Poonia, An overview on advancements in hydrogels for effective wastewater treatment, *J. Mol. Liq.*, 2025, **424**, 127120, DOI: 10.1016/j.molliq.2025.127120.
8 J. Sánchez, D. Dax, Y. Tapiero, C. Xu and S. Willför, Bio-based hydrogels with ion exchange properties applied to remove Cu(II), Cr(VI), and As(V) ions from water, *Front. Bioeng. Biotechnol.*, 2021, **9**, 656472, DOI: 10.3389/fbioe.2021.656472.
9 R. M. Trinadha, C. H. V. S. Phanindra, M. Yamini and C. H. Prasad, Hydrogels the three-dimensional networks: A review, *Int. J. Curr. Pharm. Res.*, 2021, **13**(1), 12–17, DOI: 10.22159/ijcpr.2021v13i1.40823.
10 S. L. Loo, L. Vásquez, A. Athanassiou and D. Fragouli, Polymeric Hydrogels—A promising platform in enhancing water security for a sustainable future, *Adv. Mater. Interfac.*, 2021, **8**, 2100580, DOI: 10.1002/admi.202100580.

11 T. Sandu, A.-L. Chiriac, A. Zaharia, T.-V. Iordache and A. Sarbu, New trends in preparation and use of hydrogels for water treatment, *Gels*, 2025, **11**(4), 238, DOI: 10.3390/gels11040238.
12 Z. Ahmad, S. Salman, S. A. Khan, A. Amin, Z. U. Rahman, Y. O. Al-Ghamdi, K. Akhtar, E. M. Bakhsh and S. B. Khan, Versatility of hydrogels: from synthetic strategies, classification, and properties to biomedical applications, *Gels*, 2022, **8**(3), 167, DOI: 10.3390/gels8030167.
13 M. M. E. Sayed, Production of polymer hydrogel composites and their applications, *J. Polym. Environ.*, 2023, **31**, 2855–2879, DOI: 10.1007/s10924-023-02796-z.
14 R. A. Rather, M. A. Bhat and A. H. Shalla, An insight into synthetic and physiological aspects superabsorbent hydrogels based on carbohydrate type polymers for various applications: A review, *Carbohydr. Polym. Technol. Appl.*, 2022, **3**, 100202, DOI: 10.1016/j.carpta.2022.100202.
15 X. Yin, P. Xu and H. Wang, Efficient and selective removal of heavy metals and dyes from aqueous solutions using Guipi residue-based hydrogel, *Gels*, 2024, **10**(2), 142, DOI: 10.3390/gels10020142.
16 P. Haripriya and K. Vijayakrishna, A multifaceted poly(ionic liquid)-based superabsorbent hydrogel for simultaneous removal of heavy metals and synthetic dyes, *Polym. Chem.*, 2025, **16**(34), 3875–3885, DOI: 10.1039/D5PY00584A.
17 S. Lone, D. H. Yoon, H. Lee and I. W. Cheong, Gelatin–chitosan hydrogel particles for efficient removal of Hg (II) from wastewater, *Environ. Sci.:Water Res. Technol.*, 2019, **5**, 83, DOI: 10.1039/c8ew00678d.
18 A. N. Doyo, R. Kumar and M. A. Barakat, Recent advances in cellulose, chitosan, and alginate based biopolymeric composites for adsorption of heavy metals from wastewater, *J. Taiwan Inst. Chem. Eng.*, 2023, **151**, 105095, DOI: 10.1016/j.jtice.2023.105095.
19 M. A. U. R. Qureshi, U. Farooq, M. Athar, M. Salman and N. Rehmat, *Desalin. Water Treat.*, 2017, **82**, 201–209, DOI: 10.5004/dwt.2017.21008.
20 H. Manzoor, N. Arshad, M. A. U. R. Qureshi and A. Javed, Hydroxyapatite-reinforced pectin hydrogel films PEC/PVA/APTES/HAp: doxycycline loading for sustained drug release and wound healing applications, *RSC Adv.*, 2025, **15**, 30026, DOI: 10.1039/d5ra01989c.
21 H. Chang, H. Wei, Y. Qi, S. Ding, H. Li and S. Si, Advances in hybrid hydrogel design for biomedical applications: innovations in drug delivery and tissue engineering for gynecological cancers, *Cell Biol. Toxicol.*, 2025, **41**, 115, DOI: 10.1007/s10565-025-10064-0.
22 A. Jayakumar, V. K. Jose and J. M. Lee, Hydrogels for medical and environmental applications, *Small Methods*, 2020, **4**, 1900735, DOI: 10.1002/smtd.201900735.
23 L. Li, P. Wu, F. Yu and J. Ma, Double network hydrogels for energy/environmental applications: challenges and opportunities, *J. Mater. Chem. A*, 2022, **10**, 9215–9247, DOI: 10.1039/D2TA00540A.
24 G. Jing, L. Wang, H. Yu, W. A. Amer and L. Zhang, Recent progress on study of hybrid hydrogels for water treatment, *Colloids Surf., A*, 2013, **416**, 86–94, DOI: 10.1016/j.colsurfa.2012.09.043.
25 N. Iqbal, P. Ganguly, L. Yildizbakan, E. M. Raif, E. Jones, P. V. Giannoudis and A. Jha, Chitosan scaffolds from crustacean and fungal sources: A comparative study for bone-tissue-engineering applications, *Bioengineering*, 2024, **11**, 720, DOI: 10.3390/bioengineering11070720.
26 H. Izadi, H. Asadi and M. Bemani, Chitin: a comparison between its main sources, *Front. Mater.*, 2025, **12**, 1537067, DOI: 10.3389/fmats.2025.1537067.
27 M. A. Ibrahim, M. H. Alhalafi, E. M. Emam, H. Ibrahim and R. M. Mosaad, A Review of chitosan and chitosan nanofiber: preparation, characterization, and its potential applications, *Polymers*, 2023, **15**(13), 2820, DOI: 10.3390/polym15132820.
28 M. Yadav, B. Kaushik, G. K. Rao, C. M. Srivastava and D. Vaya, Advances and challenges in the use of chitosan and its derivatives in biomedical fields: A review, *Carbohydr. Polym. Technol. Appl.*, 2023, **5**, 100323, DOI: 10.1016/j.carpta.2023.100323.
29 C. Chartier, S. Buwalda, H. V. D. Berghe, B. Nottelet and T. Budtova, Tuning the properties of porous chitosan: Aerogels and cryogels, *Int. J. Biol. Macromol.*, 2022, **202**, 215–223, DOI: 10.1016/j.ijbiomac.2022.01.042.
30 M. E. S. A. Raouf, R. K. Farag, A. A. Farag, M. Keshawy, A. A. Aziz and A. Hasan, Chitosan-Based Architectures as an Effective Approach for the Removal of Some Toxic Species from Aqueous Media, *ACS Omega*, 2023, **8**(11), 10086–10099, DOI: 10.1021/acsomega.2c07264.
31 S. G. Zielińska, Cross-Linking Agents in Three-Component Materials Dedicated to Biomedical Applications: A Review, *Polymers*, 2024, **16**(18), 2679, DOI: 10.3390/polym16182679.
32 M. M. R. Khan and M. M. H. Rumon, Synthesis of PVA-Based Hydrogels for Biomedical Applications: Recent Trends and Advances, *Gels*, 2025, **11**(2), 88, DOI: 10.3390/gels11020088.
33 C. A. G. Aldapa, G. Velazquez, M. C. Gutierrez, E. R. Vargas, J. C. Rosas and R. Y. A. Loredo, Effect of polyvinyl alcohol on the physicochemical properties of biodegradable starch films, *Mater. Chem. Phys.*, 2020, **239**, 122027, DOI: 10.1016/j.matchemphys.2019.122027.
34 Y. Zu, Y. Zhang, X. Zhao, C. Shan, S. Zu, K. Wang, Y. Li and Y. Ge, Preparation and characterization of chitosan-polyvinyl alcohol blend hydrogels for the controlled release of nano-insulin, *Int. J. Biol. Macromol.*, 2012, **50**(1), 82–87, DOI: 10.1016/j.ijbiomac.2011.10.006.
35 H. Wang, B. Tian, F. Wang, J. Zhang and Z. Wang, An efficient approach to strengthen polyvinyl alcohol physical hydrogel via in situ growing NH_2-decorated polysiloxane structures, *Mater. Lett.*, 2021, **290**, 129505, DOI: 10.1016/j.matlet.2021.129505.
36 Y. Y. Jiang, Y. J. Zhu, H. Li, Y. G. Zhang, Y. Q. Shen, T. W. Sun and F. Chen, Preparation and enhanced mechanical properties of hybrid hydrogels comprising ultralong hydroxyapatite nanowires and sodium alginate, *J. Colloid Interface Sci.*, 2017, **497**, 266–275, DOI: 10.1016/j.jcis.2017.03.032.
37 N. Asadzadeh, M. Ghorbanpour and A. Sayyah, Effects of filler type and content on mechanical, thermal, and

physical properties of carrageenan biocomposite films, *Int. J. Biol. Macromol.*, 2023, **253**, 127551, DOI: 10.1016/j.ijbiomac.2023.127551.

38 M. R. Kasaai, Nano-sized Clays, Graphene, and Inorganic Oxides as Fillers of Nanocomposites for Their Mechanical and Barrier Properties Improvement, in. *Handbook of Nanofillers*, ed S. Mallakpour and C. M. Hussain, Springer, Singapore, 2025, DOI: 10.1007/978-981-96-2407-2_149.

39 S. N. Zhumagaliyeva, R. S. Iminova, G. Z. Kairalapova, M. M. Beysebekov, M. K. Beysebekov and Z. A. Abilov, Composite Polymer-Clay Hydrogels Based on Bentonite Clay and Acrylates: Synthesis, Characterization and Swelling Capacity, *Eurasian Chem.-Technol. J.*, 2017, **19**(3), 279, DOI: 10.18321/ectj672.

40 A. A. Ali and S. Ahmed, Eco-friendly natural extract loaded antioxidative chitosan/polyvinyl alcohol based active films for food packaging, *Heliyon*, 2021, **7**(3), e06550, DOI: 10.1016/j.heliyon.2021.e06550.

41 M. Koosha and S. Hamedi, Intelligent Chitosan/PVA nanocomposite films containing black carrot anthocyanin and bentonite nanoclays with improved mechanical, thermal and antibacterial properties, *Prog. Org. Coat.*, 2019, **127**, 338–347, DOI: 10.1016/J.PORGCOAT.2018.11.028.

42 N. N. A. Malek, A. H. Jawad, K. Ismail, R. Razuan and Z. A. Alothman, Fly ash modified magnetic chitosan-polyvinyl alcohol blend for reactive orange 16 dye removal: Adsorption parametric optimization, *Int. J. Biol. Macromol.*, 2021, **189**, 464–476, DOI: 10.1016/j.ijbiomac.2021.08.160.

43 J. Jia, Y. Liu and S. Sun, Preparation and characterization of chitosan/bentonite composites for Cr (VI) removal from aqueous solutions, *Adsorpt. Sci. Technol.*, 2021, 6681486, DOI: 10.1155/2021/6681486.

44 H. Kaur, S. Singh, S. Rode, P. K. Chaudhary, N. A. Khan, P. C. Ramamurthy, D. N. Gupta, R. Kumar, J. Das and A. K. Sharma, Fabrication and characterization of polyvinyl alcohol-chitosan composite nanofibers for carboxylesterase immobilization to enhance the stability of the enzyme, *Sci. Rep.*, 2024, **14**(1), 19615, DOI: 10.1038/s41598-024-67913-x.

45 H. Chopra, S. Bibi, S. Kumar, M. S. Khan, P. Kumar and I. Singh, Preparation and Evaluation of Chitosan/PVA Based Hydrogel Films Loaded with Honey for Wound Healing Application, *Gels*, 2022, **8**(2), 111, DOI: 10.3390/gels8020111.

46 C. J. V. Alegría, R. M. F. Rivas, J. L. G. Rivas, R. E. Z. Arce, M. L. J. Núñez and B. G. Gaitán, Synthesis of Chitosan-Polyvinyl Alcohol Biopolymers to Eliminate Fluorides from Water, *Biomolecules*, 2020, **10**(1), 156, DOI: 10.3390/biom10010156.

47 H. J. Rao, Characterization Studies on Adsorption of Lead and Cadmium Using Activated Carbon Prepared from Waste Tyres, *Nat. Environ. Pollut. Technol.*, 2021, **20**(2), 561–568, DOI: 10.46488/NEPT.2021.v20i02.012.

48 G. Sharma, A. Kumar, A. A. Ghfar, A. G. Peñas, M. Naushad and F. J. Stadler, Fabrication and Characterization of Xanthan Gum-cl-poly (acrylamide-co-alginic acid) Hydrogel for Adsorption of Cadmium Ions from Aqueous Medium, *Gels*, 2021, **8**(1), 23, DOI: 10.3390/gels8010023.

49 M. A. U. R. Qureshi, N. Arshad and A. Rasool, Graphene oxide reinforced biopolymeric (chitosan) hydrogels for controlled cephradine release, *Int. J. Biol. Macromol.*, 2023, **242**, 124948, DOI: 10.1016/j.ijbiomac.2023.124948.

50 X. Zhong, H. Jian, G. Dou, J. Liu and H. Tan, Preparation and Characterization of a Bentonite-Based Hybrid Gel for Coal Spontaneous Combustion Prevention, *ACS Omega*, 2022, **7**(50), 46536–46549, DOI: 10.1021/acsomega.2c05359.

51 R. S. Hebbar, A. M. Isloor, B. Prabhu, Inamuddin, A. M. Asiri and A. F. Ismail, Removal of metal ions and humic acids through polyetherimide membrane with grafted bentonite clay, *Sci. Rep.*, 2018, **8**, 4665, DOI: 10.1038/s41598-018-22837-1.

52 M. H. Ali, M. A. K. Azad, K. A. Khan, M. O. Rahman, U. Chakma and A. Kumer, Analysis of Crystallographic Structures and Properties of Silver Nanoparticles Synthesized Using PKL Extract and Nanoscale Characterization Techniques, *ACS Omega*, 2023, **8**(31), 28133–28142, DOI: 10.1021/acsomega.3c01261.

53 X. Ning, J. Huang, A. Yimuhan, N. Yuan, C. Chen and D. Lin, Research Advances in Mechanical Properties and Applications of Dual Network Hydrogels, *Int. J. Mol. Sci.*, 2022, **23**(24), 15757, DOI: 10.3390/ijms232415757.

54 G. Michailidou, N. Ainali, E. Xanthopoulou, S. Nanaki, M. Kostoglou, E. Koukaras and D. Bikiaris, Effect of Poly (vinyl alcohol) on Nanoencapsulation of Budesonide in Chitosan Nanoparticles via Ionic Gelation and Its Improved Bioavailability, *Polymers*, 2020, **12**(5), 1101, DOI: 10.3390/polym12051101.

55 X. Guo, Z. Wu, Z. Wang, F. Lin, P. Li and J. Liu, Preparation of Chitosan-Modified Bentonite and Its Adsorption Performance on Tetracycline, *ACS Omega*, 2023, **8**(22), 19455–19463, DOI: 10.1021/acsomega.3c00745.

56 H. Huo, J. Shen, J. Wan, H. Shi, H. Yang, X. Duan, Y. Gao, Y. Chin, F. Kuang, H. Li, L. Yang and G. Du, A tough and robust hydrogel constructed through carbon dots induced crystallization domains integrated orientation regulation, *Nat. Commun.*, 2025, **16**, 6221, DOI: 10.1038/s41467-025-61535-1.

57 S. Wang, Y. Liu, A. Yang, Q. Zhu, H. Sun, P. Sun, B. Yao, Y. Zang, X. Du and L. Dong, Xanthate-Modified Magnetic Fe_3O_4@SiO_2-Based Polyvinyl Alcohol/Chitosan Composite Material for Efficient Removal of Heavy Metal Ions from Water, *Polymers*, 2022, **14**(6), 1107, DOI: 10.3390/polym14061107.

58 S. Khodami, K. Kaniewska, J. Romanski, M. Karbarz and Z. Stojek, Amino Acid-Based Hydrogel with Interpenetrating Gelatin and Cross-Linked by Metal Ions, Providing High Stretchability and Motion Sensitivity, *ACS Omega*, 2025, **10**(12), 12062–12075, DOI: 10.1021/acsomega.4c10083.

59 R. Mu, B. Liu, X. Chen, N. Wang and J. Yang, Hydrogel adsorbent in industrial wastewater treatment and ecological environment protection, *Environ. Technol. Innov.*, 2020, **20**, 101107, DOI: 10.1016/j.eti.2020.101107.

60 M. T. A. Samman and J. Sánchez, Chitosan- and Alginate-Based Hydrogels for the Adsorption of Anionic and

Cationic Dyes from Water, *Polymers*, 2022, **14**(8), 1498, DOI: 10.3390/polym14081498.

61 P. Beigi, F. Ganjali, F. H. Afruzi, M. M. Salehi and A. Maleki, Enhancement of adsorption efficiency of crystal violet and chlorpyrifos onto pectin hydrogel@Fe_3O_4-bentonite as a versatile nanoadsorbent, *Sci. Rep.*, 2023, **13**, 10764, DOI: 10.1038/s41598-023-38005-z.

62 Z. Lin, Y. Yang, Z. Liang, L. Zeng and A. Zhang, Preparation of Chitosan/Calcium Alginate/Bentonite Composite Hydrogel and Its Heavy Metal Ions Adsorption Properties, *Polymers*, 2021, **13**(11), 1891, DOI: 10.3390/polym13111891.

63 W. Wang, X. Liu, X. Wang, L. Zong, Y. Kang and A. Wang, Fast and Highly Efficient Adsorption Removal of Toxic Pb(II) by a Reusable Porous Semi-IPN Hydrogel Based on Alginate and Poly (vinyl alcohol), *Front. Chem.*, 2021, **9**, 662482, DOI: 10.3389/fchem.2021.662482.

64 L. A. Shah, H. Subhan, S. Alam, D. Ye and M. Ullah, Bentonite clay reinforced alginate grafted composite hydrogel with remarkable sorptive performance toward removal of methylene green, *Int. J. Biol. Macromol.*, 2024, **279**(4), 135600, DOI: 10.1016/j.ijbiomac.2024.135600.

65 W. Liu, Y. Zhang, S. Wang, L. Bai, Y. Deng and J. Tao, Effect of Pore Size Distribution and Amination on Adsorption Capacities of Polymeric Adsorbents, *Molecules*, 2021, **26**(17), 5267, DOI: 10.3390/molecules26175267.

66 M. M. Bhuyan and M. Ahmed, Effective Hydrogel Surfaces for Adsorption of Pharmaceutical and Organic Pollutants—A Mini Review, *Surfaces*, 2025, **8**(3), 61, DOI: 10.3390/surfaces8030061.

67 B. Thakur, G. Sharma, A. Kumar, S. Sharma, M. Naushad, J. Iqbal and F. J. Stadler, Designing of bentonite based nanocomposite hydrogel for the adsorptive removal and controlled release of ampicillin, *J. Mol. Liq.*, 2020, **319**, 114166, DOI: 10.1016/j.molliq.2020.114166.

68 A. Ilseng, V. Prot, B. H. Skallerud and B. T. Stokke, Buckling initiation in layered hydrogels during transient swelling, *J. Mech. Phys. Solid.*, 2019, **128**, 219–238, DOI: 10.1016/j.jmps.2019.04.008.

69 S. D. Chaudhuri, A. Dey, S. Upganlawar and D. Chakrabarty, Influence of clay concentration on the absorption and rheological attributes of modified cellulose/acrylic acid based hydrogel and the application of such hydrogel, *Mater. Chem. Phys.*, 2022, **282**, 125942, DOI: 10.1016/j.matchemphys.2022.125942.

70 Z. H. Ghauri, A. Islam, M. A. Qadir, N. Gull, B. Haider, R. U. Khan and T. Riaz, Development and evaluation of pH-sensitive biodegradable ternary blended hydrogel films (chitosan/guar gum/PVP) for drug delivery application, *Sci. Rep.*, 2021, **11**, 21255, DOI: 10.1038/s41598-021-00452-x.

71 T. M. T. Vo, T. Piroonpan, C. Preuksarattanawut, T. Kobayashi and P. Potiyaraj, Characterization of pH-responsive high molecular-weight chitosan/poly (vinyl alcohol) hydrogel prepared by gamma irradiation for localizing drug release, *Bioresour. bioprocess.*, 2022, **9**, 89, DOI: 10.1186/s40643-022-00576-6.

72 M. U. A. Khan, I. Iqbal, M. N. M. Ansari, S. I. A. Razak, M. A. Raza, A. Sajjad, F. Jabeen, M. R. Mohamad and N. Jusoh, Development of Antibacterial, Degradable and pH-Responsive Chitosan/Guar Gum/Polyvinyl Alcohol Blended Hydrogels for Wound Dressing, *Molecules*, 2021, **26**(19), 5937, DOI: 10.3390/.molecules26195937.

73 Z. Megrelishvili, I. Didmanidze, N. Dondoladze, T. Jojua, L. Bestaeva and D. Chkhubiani, Study of the processes of sorption and ion exchange of bentonite clays of Georgia, *Appl. Chem. Eng.*, 2025, **8**(1), 10, DOI: 10.59429/ace.v8i1.5628.

74 H. Zhang, Y. Shi, X. Xu, M. Zhang and L. Ma, Structure Regulation of Bentonite-Alginate Nanocomposites for Controlled Release of Imidacloprid, *ACS Omega*, 2020, **5**(17), 10068–10076, DOI: 10.1021/acsomega.0c00610.

75 M. Arvand and M. Pakseresht, Cadmium adsorption on modified chitosan-coated bentonite: batch experimental studies, *J. Chem. Technol. Biotechnol.*, 2013, **88**, 572–578, DOI: 10.1002/JCTB.3863.

76 W. Ding, H. Liang, H. Zhang, H. Sun, Z. Geng and C. Xu, A cellulose/bentonite grafted polyacrylic acid hydrogel for highly-efficient removal of Cd (II), *J. Water Proc. Eng.*, 2023, **51**, 103414, DOI: 10.1016/j.jwpe.2022.103414.

77 Y. Dehmani, I. Bentahar, H. Lgaz, A. El-Kordy, A. Aldalbahi, A. A. Alrashdi, A. Dehbi, T. Lamhasni, B. Hammouti and A. Sadik, A critical review of natural clay minerals: Structural characterization, textural properties, and adsorption mechanisms for sustainable wastewater treatment, *Mater. Today Adv.*, 2026, **29**, 100682, DOI: 10.1016/j.mtadv.2025.100682.

78 N. Hodzic, A. Djozic, I. Šestan and H. Alihodžić, Examination of Adsorption Abilities of Natural and Acid Activated Bentonite for Heavy Metals Removal from Aqueous Solutions, *Int. J. Res. Appl. Sci. Biotechnol.*, 2020, **7**(1), 1–6, DOI: 10.31033/ijrasb.7.1.1.

79 C. Huang, Y. Huang, T. Xie, W. Yu and S. Ai, Adsorption Mechanism of Bentonite with Dispersed Chitosan for Cadmium Ions, *Chem. Eng. Technol.*, 2021, **44**, 441–448, DOI: 10.1002/ceat.202000505.

80 M. Arvand and M. A. Pakseresht, Cadmium adsorption on modified chitosan-coated bentonite: batch experimental studies, *J. Chem. Technol. Biotechnol.*, 2013, **88**, 572–578, DOI: 10.1002/jctb.3863.

81 P. B. Vilela, C. A. Matias, A. Dalalibera, V. A. Becegato and A. T. Paulino, Polyacrylic acid-based and chitosan-based hydrogels for adsorption of cadmium: Equilibrium isotherm, kinetic and thermodynamic studies, *J. Environ. Chem. Eng.*, 2019, **7**(5), 103327, DOI: 10.1016/J.JECE.2019.103327.

82 T. F. Akinhanmi, E. A. Ofudje, A. I. Adeogun, P. Aina and I. M. Joseph, Orange peel as low-cost adsorbent in the elimination of Cd (II) ion: kinetics, isotherm, thermodynamic and optimization evaluations, *Bioresour. bioprocess.*, 2020, **7**, 34, DOI: 10.1186/s40643-020-00320-y.

83 M. A. A. Aljar, S. Rashdan, A. Almutawah and A. A. E. Fattah, Synthesis and Characterization of Biodegradable Poly (vinyl alcohol)-Chitosan/Cellulose Hydrogel Beads for Efficient Removal of Pb(II), Cd (II), Zn(II), and Co(II) from Water, *Gels*, 2023, **9**(4), 328, DOI: 10.3390/gels9040328.

84 R. E. K. Billah, I. Ayouch, Y. Abdellaoui, Z. Kassab, M. A. Khan, M. Agunaou, A. Soufiane, M. Otero and B. H. Jeon, A Novel Chitosan/Nano-Hydroxyapatite Composite for the Adsorptive Removal of Cd (II) from Aqueous Solution, *Polymers*, 2023, **15**(6), 1524, DOI: 10.3390/polym15061524.

85 P. Pal and A. Pal, Surfactant-modified chitosan beads for cadmium ion adsorption, *Int. J. Biol. Macromol.*, 2017, **104**(B), 1548–1555, DOI: 10.1016/j.ijbiomac.2017.02.042.

86 M. R. Abukhadra, N. Nasser, A. M. El-Sherbeeny and W. A. Zoubi, Enhanced Retention of Cd (II) by Exfoliated Bentonite and Its Methoxy Form: Steric and Energetic Studies, *ACS Omega*, 2024, **9**(10), 11534–11550, DOI: 10.1021/acsomega.3c08592.

87 C. Li, Y. Yan, Q. Zhang, Z. Zhang, L. Huang, J. Zhang, Y. Xiong and S. Tan, Adsorption of Cd2+ and Ni2+ from Aqueous Single-Metal Solutions on Graphene Oxide-Chitosan-Poly (vinyl alcohol) Hydrogels, *Langmuir*, 2019, **35**(13), 4481–4490, DOI: 10.1021/acs.langmuir.8b04189.

88 N. B. Milosavljević, M. D. Ristić, A. A. P. Grujić, J. M. Filipović, S. B. Štrbac, Z. L. Rakočević and M. T. K. Krušić, Hydrogel based on chitosan, itaconic acid and methacrylic acid as adsorbent of $Cd2^{+}$ ions from aqueous solution, *Chem. Eng. J.*, 2010, **165**(2), 554–562, DOI: 10.1016/j.cej.2010.09.072.

89 A. Babakhani and M. Sartaj, Removal of Cadmium (II) from aqueous solution using tripolyphosphate cross-linked chitosan, *Environ. Chem. Eng.*, 2020, **8**(4), 103842, DOI: 10.1016/j.jece.2020.103842.

90 Y. M. Desalegn, E. A. Bekele and F. E. Olu, Optimization of Cd (II) removal from aqueous solution by natural hydroxyapatite/bentonite composite using response surface methodology, *Sci. Rep.*, 2023, **13**, 5158, DOI: 10.1038/s41598-023-32413-x.

91 Q. U. Ain, H. Zhang, M. Yaseen, U. Rasheed, L. Kun, S. Subhan and Z. Tong, Facile fabrication of hydroxyapatite-magnetite-bentonite composite for efficient adsorption of Pb(II), Cd (II), and crystal violet from aqueous solution, *J. Clean. Prod.*, 2020, **247**, 119088, DOI: 10.1016/j.jclepro.2019.119088.

92 I. Esmaeili, F. Soltanolkottabi, F. Hosseini and H. Jafari, Investigation of cadmium adsorption factors from water by synthesis of chitosan/polyvinyl alcohol/modified FDU-12 nanocomposite, *J. Chin. Chem. Soc.*, 2024, **71**(2), 197–208, DOI: 10.1002/jccs.202300332.

93 A. Heidari, H. Younesi, Z. Mehraban and H. Heikkinen, Selective adsorption of Pb(II), Cd(II), and Ni(II) ions from aqueous solution using chitosan-MAA nanoparticles, *Int. J. Biol. Macromol.*, 2013, **61**, 251–263, DOI: 10.1016/j.ijbiomac.2013.06.032.

94 S. Wang, Y. Wang, X. Wang, S. Sun, Y. Zhang, W. Jiao and D. Lin, Study on Adsorption of Cd in Solution and Soil by Modified Biochar–Calcium Alginate Hydrogel, *Gels*, 2024, **10**(6), 388, DOI: 10.3390/gels10060388.

95 W. Yang, W. Luo, T. Sun, Y. Xu and Y. Sun, Adsorption Performance of Cd(II) by Chitosan-Fe_3O_4-Modified Fish Bone Char, *Int. J. Environ. Res. Publ. Health*, 2022, **19**(3), 1260, DOI: 10.3390/ijerph19031260.